Bulletin of the JSME Vol.9, No.3, 2014
Journal of Fluid Science and Technology

Study on flow around straight-bladed vertical axis wind turbine under low tip speed ratio

Qing'an LI*, Takao MAEDA*, Yasunari KAMADA*, Junsuke MURATA*,
Toshiaki KAWABATA* and Tetsuya KOGAKI**
* Graduate School of Engineering, Mie University
1577 Kurimamachiya-cho, Tsu-shi, Mie 514-8507, Japan
E-mail: li@fel.mach.mie-u.ac.jp
** National Institutes of Advanced Industrial Science and Technology
1-2-1 Namiki, Tsukuba-shi, Ibaraki 305-8564, Japan

Received 27 February 2014

Abstract
The flow field around a vertical axis wind turbine (VAWT) is very complicated because the blades pass in non-uniform flow field by the blade wake during rotation. There is some difficulty in measuring the aerodynamics acting on VAWT at a low tip speed ratio during rotation, because the relative wind speed and the angle of attack for the blade are periodically changing. So few experimental data are available for the low tip speed ratio compared with the high tip speed ratio. This paper presents a method for wind velocity distribution around VAWT at low tip speed ratios. According to this research, the flow field around a straight-bladed VAWT which has three blades is analyzed. The wind velocity in flow field is measured by using the Laser Doppler Velocimeter (LDV) in wind tunnel, and the wind velocity distribution is obtained under different azimuth angles. Flow field characteristics are also investigated for several values of tip speed ratio. Firstly, a wide low wind velocity field appears from the wind turbine internal region to downstream region. Secondly, from upstream to downstream region, the velocity deficit has become greater in the mainstream direction, at the same time, the reverse flow is only generated in the back of the cover of the rotation axis at optimum tip speed ratio. Finally, large turbulence intensity is generated at the inside of wind turbine.

Key words : Vertical axis wind turbine (VAWT), Flow field, Low tip speed ratio, Laser Doppler Velocimeter (LDV), Velocity deficit, Turbulence intensity

1. Introduction

Strong growth of utilizing wind energy in the past decade stimulates extensive research efforts on the wind turbine technology nowadays. According to the direction of rotor axis, wind turbines are classified into two categories: Horizontal Axis Wind Turbine (HAWT) and Vertical Axis Wind Turbine (VAWT). The main advantage of VAWT is that no yaw mechanisms are required. Blades of straight-bladed VAWT are uniform section and non-twisted, so this makes them relatively easy to fabricate or extrude (Asress, et al., 2013). VAWT is expected to provide power for portable device, crisis evacuation indicator in disaster events, etc. However, compared with the HAWT，the simple design techniques still have not been developed due to lack of the basic data.

The critical disadvantage of VAWT is that the flow field characteristics are very complicated during rotation, because the angles of attack for the blade and relative flow velocity are periodically changing (Mazharul, et al., 2008), especially at low tip speed ratio. Furthermore, several dynamic effects such as dynamic stall can affect the aerodynamic loading of the blade (Rajat, et al., 2010). So that it makes more difficult to analyze the aerodynamic characteristics of VAWT at low tip speed ratio (Castelli, et al., 2012). Therefore, it is a major challenge to analyze the characteristics of flow field and aerodynamic behavior of small straight-bladed VAWT during rotation at low tip speed ratio and to improve the aerodynamic performance.

In recent years, many researches on straight-bladed VAWT have been carried out around the world. For predicting

Paper No.14-00091
[DOI: 10.1299/jfst.2014jfst0051]
© 2014 The Japan Society of Mechanical Engineers

wind turbine flow field, Fujisawa, et al. studied the formation and development of dynamic stall around blade by using flow visualization and instantaneous velocity measurement by particle image velocimetry (PIV) technology (Fujisawa and Shibuya, 2001). To make the prediction more efficient, aerodynamic behavior of a vertical axis wind turbine (VAWT) is analyzed by means of PIV, focusing on the development of dynamic stall around blade at different tip speed ratios (Ferreira, et al., 2009). Several authors also focused on CFD analysis of the aerodynamics and flow field. For example, Sato, et al compared the analysis of flows around straight-bladed VAWT with two blades between wind tunnel by hotwire measurements and numerical simulations (Sato, et al., 2011). However, analysis of the flow field, especially when it is operating at low tip speed ratio in wind tunnel, is still one of the most difficult problems in fluid engineering. Specifically, there have been few reports relevant to the direct measurement of the whole flow field of straight-bladed VAWT by LDV system in the experiments.

The VAWT has an unsteady aerodynamic behaviour due to the variation with the azimuth angle of the blade's angle of attack (Maeda, et al., 2013), perceived velocity. Then, the change of flow field is an inherent effect of the operation of a VAWT at low tip speed ratio, impacting both loads and power. Therefore, it is important to study the flow field around straight-bladed VAWT. In this research, to compile the assessment of flow field around the whole of small straight-bladed VAWT, the wind velocities are measured through LDV system at three different low tip speed ratios in the wind tunnel experiment.

2. Notations

C : Blade chord length (=0.265) [m]
C_p : Power coefficient ($=Q\omega/(0.5\rho DHU_0^3)$)
D : Rotor diameter (=1.0) [m]
H : Height of rotor (=1.2) [m]
N : Number of blade (=3)
Q : Rotor torque [N·m]
R : Rotor radius (=0.5) [m]
U_0 : Mainstream wind velocity (=8.5) [m/s]
U_x : x component of wind velocity [m/s]
U_y : y component of wind velocity [m/s]
w : Relative flow velocity [m/s]
x : Longitudinal coordinate [m]
y : Lateral coordinate [m]
z : Vertical coordinate [m]
β : Blade pitch angle (=10) [deg]
λ : Tip speed ratio ($=R\omega/U_0$)
θ : Azimuth angle [deg]
ρ : Air density [kg/m^3]
σ : Standard deviation of local wind velocity [m/s]
ω : Angular velocity of rotor [rad/s]

3. Experimental apparatus and method

3.1 Wind tunnel and test wind turbine

Torque is measured by torque meter, and then, wind velocity around wind turbine in flow field is measured by LDV as shown in Fig. 1. The capacity of torque sensor is 20 N m, minimum resolution is 10 mN m and accuracy is ± 0.2% at full scale. The rotational speed is ranged approximately from 0 to 6000 rpm and the moment of inertia is 5.00 × 10^{-5} kg m^2. The maximum output of LDV is 4W. The signal from the photo diode is fed into a current amplifier and amplified by a factor of 10^4.

And the schematic diagram of experimental apparatus is shown in Fig. 2. The experiments are carried out in wind tunnel with outlet diameter of 3600 mm. Tested wind turbine has a three-bladed rotor. The diameter of rotor is 1000 mm, the height of blade is 1200 mm, and the length of blade chord is 265 mm. Cross-sectional shape of airfoil is NACA0021 shown in Fig. 3. Pitot tube is installed in the upstream of 2070 mm from rotor axis. The coordinate system is defined for the measurements, in which the x-, the y- and the z-axes are set in the mainstream, the lateral and the vertical directions, respectively. The origin is taken at the center height location of wind turbine rotor. The focus of LDV is set at center height of the blade.

3.2 Experimental methods

3.2.1 Measuring range

The experimental method takes advantage of LDV to measure the wind velocity in the flow field at three different

[DOI: 10.1299/jfst.2014jfst0051]
© 2014 The Japan Society of Mechanical Engineers

low tip speed ratios (λ = 0.64, 1.03 and 1.27) during rotation. The range of the experiment covers the entire rotation of the blade and almost the entire rotor area. As shown in Fig.4, the measuring points of flow velocity are as follows: in the center height of airfoil direction (z/R = 0); in the mainstream flow direction there are eight cross-sections (x/R= -3.0, -1.5, -1.0, -0.5, 0, 0.5, 1.0, and 1.5); in y axis direction, the distance is evenly distributed at y/R = 0.2 in the range of -1.2 $\leq y/R \leq$ 1.2. However, the axis of rotation of the tested wind turbine is covered with a cylindrical cover of 216 mm diameter, so that in this range the measurement is not performed. The number of sampling data is 10000 at every measurement position and the accuracy is ±0.05%.

3.2.2 Measuring conditions

Experiments are carried out under the conditions that the mainstream velocity of U_0 = 8.5 m/s, and blade pitch angle of β = 10 °, for which wind turbine has the highest power output. As can be seen in Fig. 5, β is the blade pitch angle, which is between chord line and locus of rotor rotation. Wherein, direction in which the leading edge of airfoil outward is positive. Azimuth angle θ, on the position where the travelling direction of blade matches the mainstream

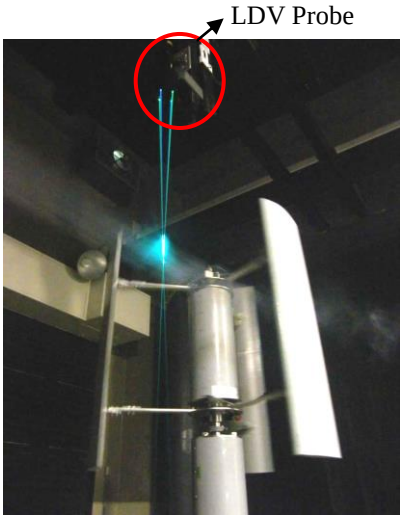


Fig. 1 LDV Measurement of Wind Velocity around VAWT Rotor in Flow Field. LDV probe is attached to a three-dimensional positioning device which set up on the upper part of the test section. The LDV creates a fringe pattern on the measured object (interference figure) using two coherent laser beams.

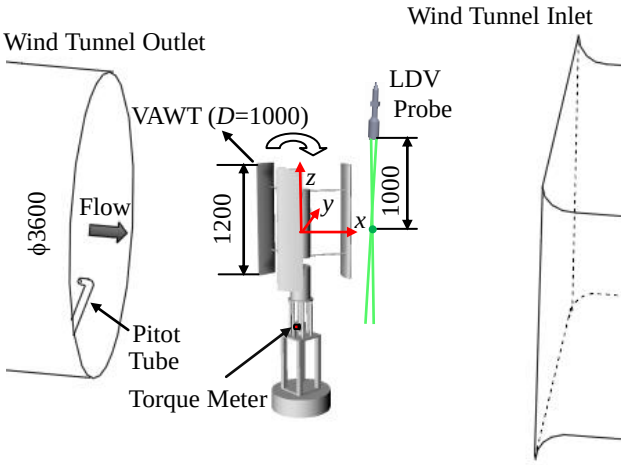


Fig. 2 Experimental Apparatus. The wind tunnel has an outlet diameter of 3600 [mm] and its maximum wind velocity reaches 30 [m/s]. LDV probe is set at 1000 [mm] from the center height of blade. The origin of coordinate system is set at the center height location of wind turbine rotor. Tested wind turbine has a three-bladed

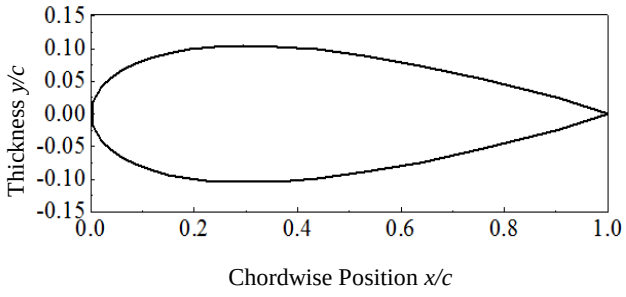


Fig. 3 Geometry of Airfoil. Cross-sectional shape of the airfoil is the same as NACA0021. The horizontal and vertical axes represent the chordwise position x/c, and the thickness y/c, respectively.

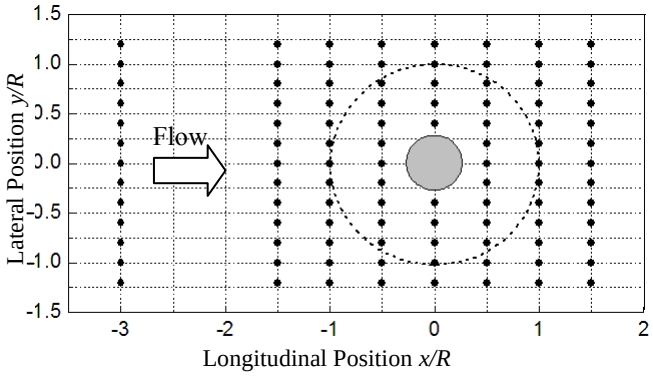


Fig. 4 Position of Measuring Points. The flow is from left to right. Small solid circle at x/R=0 and y/R=0, shows the cover portion of axis of rotation, and large broken circle shows rotor rotational trajectory.

[DOI: 10.1299/jfst.2014jfst0051]
© 2014 The Japan Society of Mechanical Engineers

direction (the negative direction of x), is defined as 0 ° as shown in Fig.6. Here, θ is specified as a positive direction in the direction of rotor rotation. In addition, velocity vector is obtained by averaged flow velocity, at each azimuth angle of 5 °BIN during one rotation.

In this experiment, the averaged x-axis and y-axis velocities are used in the following discussions. The z-axis velocities are not considered because these values are much lower than x-axis and y-axis ones at blade center height.

4. Results and discussion

4.1 Power coefficient curve

Torque meter is installed in wind turbine axis of rotation, which can determine rotor rotating speed and rotor torque. Wind turbine rotor performance is usually characterized by its power coefficient, C_p:

$$C_p = \frac{Q\omega}{0.5\rho A U_0^3} \tag{1}$$

where ρ is the density of the air, Q is the rotor torque, and A is the swept area of the turbine(=DH). The power coefficient represents the aerodynamic efficiency of the wind turbine and is a function of the tip speed ratio,λ, which is defined as

$$\lambda = \frac{R\omega}{U_0} \tag{2}$$

Wind turbine power coefficient is shown in Fig. 7. From the figure, the optimum power coefficient of 0.153 is obtained at λ = 1.03. It can be seen that power coefficient decreases gradually in accordance with the increases of tip speed ratio over optimum tip speed ratio. Power coefficient decreases with the decrease of λ below optimum tip speed

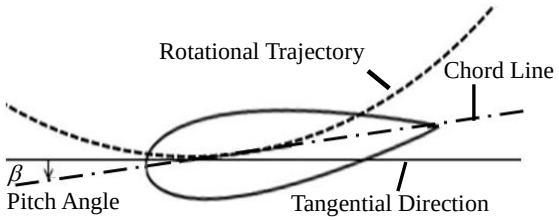


Fig. 5 Definition of Pitch Angle. Dotted line represents the chord line. The direction of blade pitch angle in which the leading edge of airfoil outward is positive.

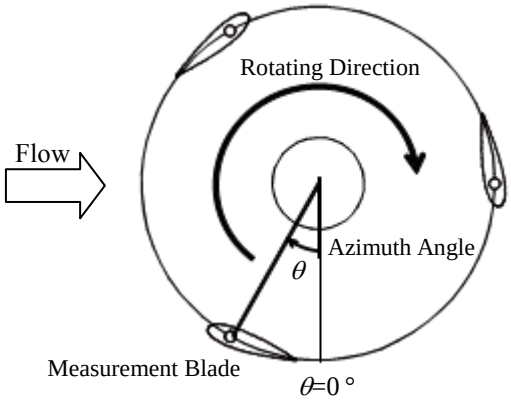


Fig. 6 Definition of Azimuth Angle. θ is specified as a positive direction from 0 ° and the same direction as rotating direction.

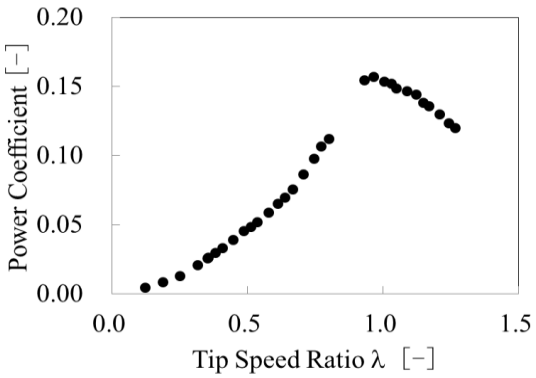


Fig. 7 Power Coefficient Curve. In the range of 0.81< λ <0.92, the power coefficient could not be obtained owning to the resonance.

[DOI: 10.1299/jfst.2014jfst0051]
© 2014 The Japan Society of Mechanical Engineers

ratio. The data acquisition for the wind turbine could not be obtained owning to the resonance in the range of $0.81< \lambda <0.92$. The reason of resonance is that the blade natural frequency equates to the rotational frequency or a harmonic with a significant forcing load. Therefore, in the course of blade design and experiment, it is important to avoid the occurrence of the resonant condition.

4.2 Flow field at optimum tip speed ratio

Figures 8(a)-(d) represent wind velocity variation of each measurement point at optimum tip speed ratio when blade passes through 0 °, 30 °, 60 ° and 90 °, respectively. The horizontal and vertical axes represent the non-dimensional longitudinal coordinate, *x/R*, and the non-dimensional lateral coordinate, *y/R*. In this figure, small solid circle at *x/R*=0 and *y/R*=0, shows the cover portion of axis of rotation, and large broken line circle shows rotor rotational trajectory. Rotational direction of rotor is clockwise. The reverse flow is generated in the back of the cover of the rotation axis space (*x/R*=0.5, *y/R*=0 and -0.2). The relative velocity around rotor becomes larger. It is seemed that the relative velocity is caused partly by the induced velocities from the bound vortices around the blades and the shed vortices and the relative motion of the blade to the undisturbed flow also gives large effects to the relative velocity. Furthermore, the induced velocities by bound vortices around the blades change with the distance between the measuring point and the rotor blades. In some cases, the magnitude of the velocity relative to the rotor blade is larger at far upstream than the vicinity of the blade.

Figure 9 shows the fluctuations of mainstream wind velocity in upstream at longitudinal position *x/R*= -0.5 at several lateral positions in condition of optimum tip speed ratio of λ=1.03. The vertical and horizontal axes represent the BIN averaged non-dimensional wind velocity U_x/U_0 and the azimuth angle θ of wind turbine. There is a periodical change of the velocity in the flow field in the mainstream direction, which is composed of three cycles in one rotor

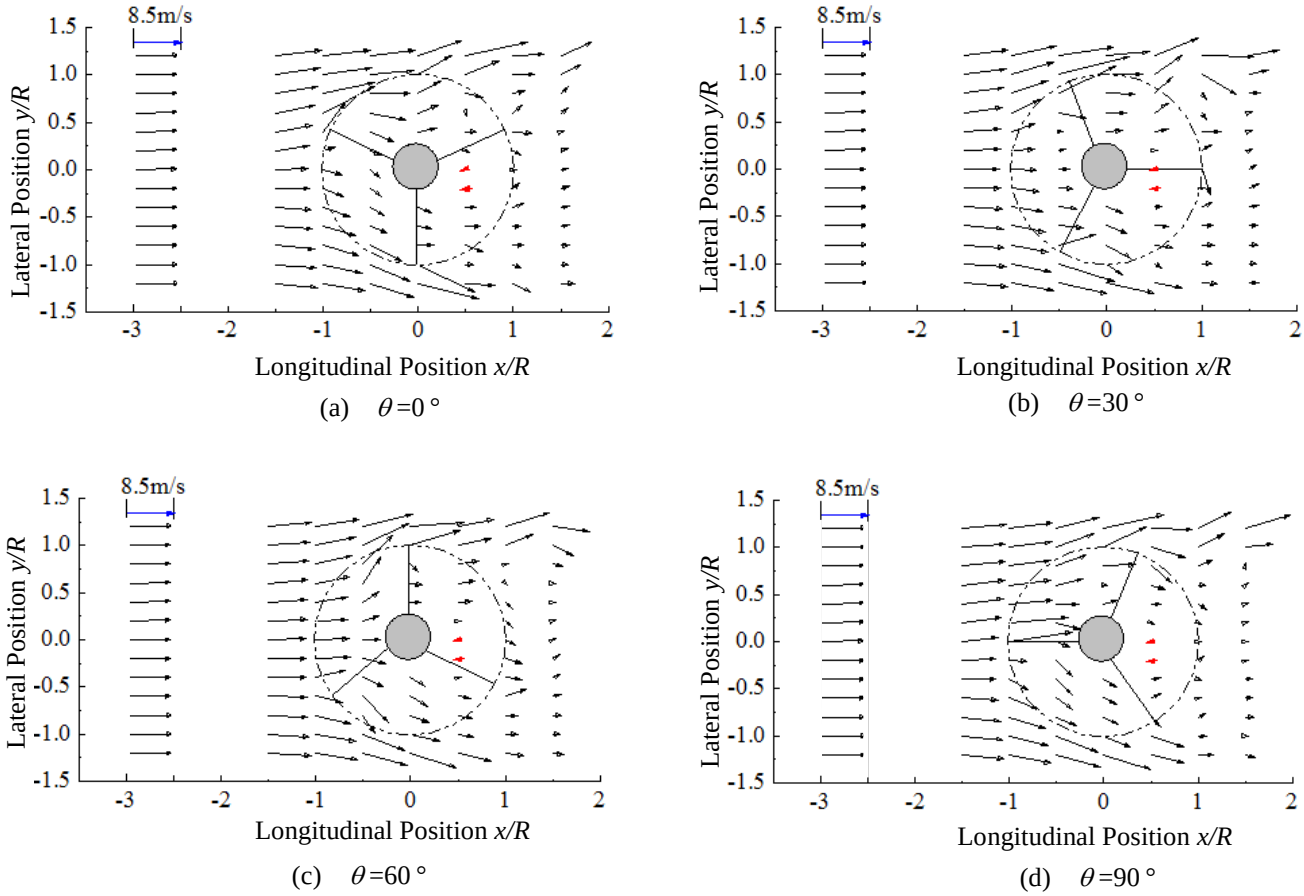


Fig. 8 Velocity Distribution for Various Azimuth Angle (Optimum Tip Speed Ratio λ=1.03). One division of scale (the blue arrow) in horizontal axis corresponds to the mainstream wind velocity of U_0= 8.5m/s. The length and direction of the arrows represent the value and direction of wind velocity, respectively.

[DOI: 10.1299/jfst.2014jfst0051]
© 2014 The Japan Society of Mechanical Engineers

revolution. In addition, the fluctuation amplitudes are the largest around y/R=1.0 where the blade tips pass. The fluctuations show almost opposite peaks at inner (y/R=0 and 0.4) and outer (y/R=1.0 and 1.2) regions of the rotor because the approach and passage of induced velocities are generated by three blades. Furthermore, fluctuation amplitudes within the rotor radius present the tendency of increase with increasing y-axis, at the same time, the azimuth angle corresponding to the maximum amplitude of U_x/U_0 also has been delayed. The magnitude of the mainstream wind velocity increases with increase of x/R and will become the largest at the tip region.

Figure 10 depicts stream-wise wind velocity U_x (x component of wind velocity). Velocity profile has an asymmetry with respect to the x-axis at the downstream side of the rotor owning to the influence of the rotation of rotor blades. Moreover, in the region of y/R>1.0, wind velocity is larger than in the region of y/R< -1.0. In addition, the wind velocity at outer regions of the rotor is larger than mainstream wind velocity of 8.5m/s. Then, the deficit area is almost symmetrical expansion with the increase of x/R. Near the wind turbine (x/R≤1.0), the velocity distribution shows a small peak around the x-axis because of the displacement effect of the rotor axis.

Figure 11 describes the lateral-wise wind velocity U_y (y component of wind velocity). The velocity increases within the rotary track. It is smaller than the stream-wise wind velocity. However, according to experimental data, in the lateral component (U_y), it is shown higher turbulence intensity than in the stream-wise component (U_x). On the other hand, it is worth noting that the velocity variation is recovered in short distance in the wake (x/R=1.5)

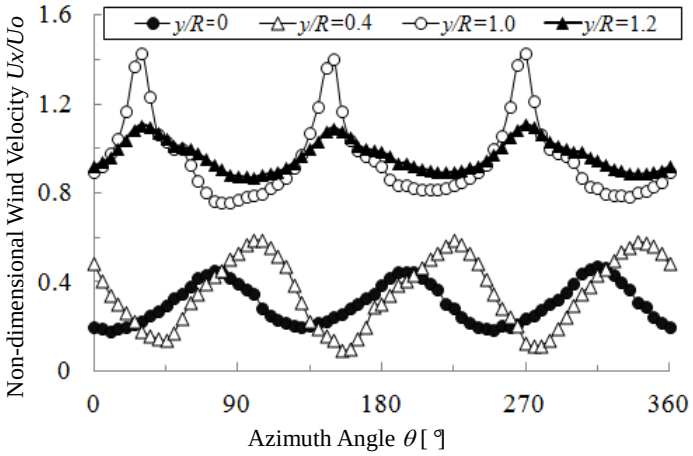
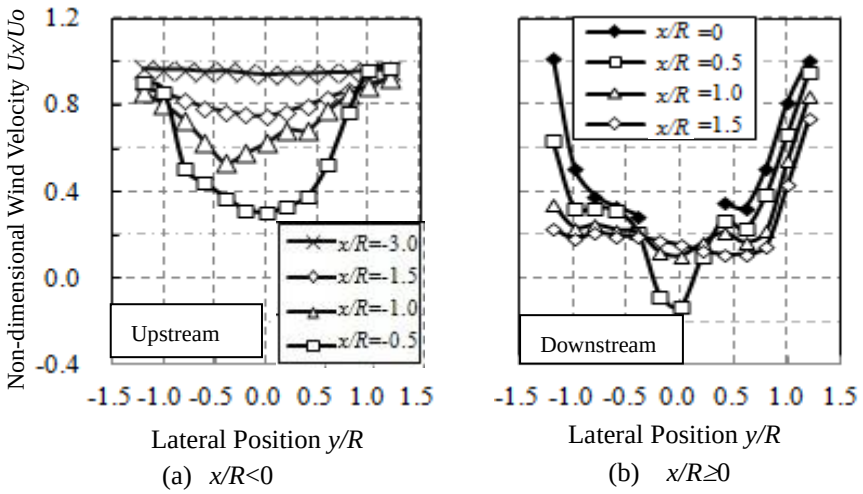


Fig. 9 Fluctuation of Wind Velocity (x/R= -0.5, λ=1.03). The two curves in the upside present fluctuation amplitudes at outer regions of the rotor (y/R=1.0 and y/R=1.2). However, the two curves in the downside present fluctuation amplitudes at inner regions of the rotor (y/R= 0 and y/R= 0.4).



(a) x/R<0 (b) x/R≥0

Fig. 10 Stream-wise Absolute Velocity Distribution (λ=1.03). Velocity profile is divided into two regions: upstream region (x/R< 0) and downstream region (x/R≥ 0). The vertical axe represents the non-dimensional wind velocity U_x/U_0 during the BIN averaged flow field.

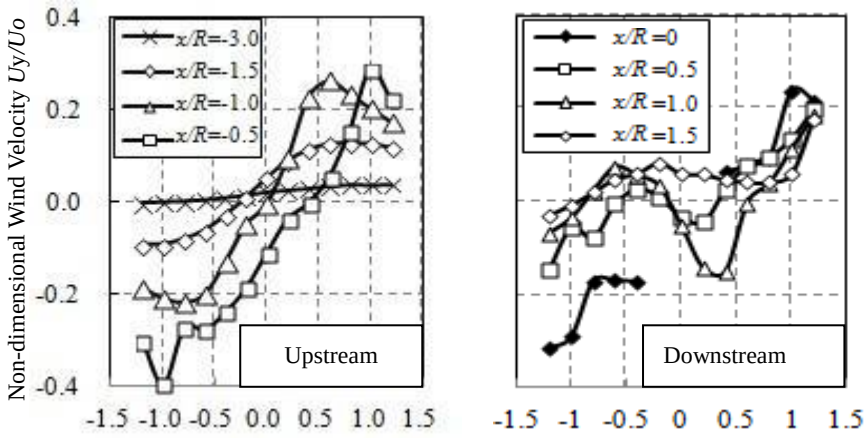
[DOI: 10.1299/jfst.2014jfst0051]
© 2014 The Japan Society of Mechanical Engineers

compared with stream-wise wind velocity. It seems that the turbulence enables a quick recovery of the wake velocity. These effects are caused by the high turbulence intensity promoting the entrainment of the main flow and wake.

4.3 Comparison of flow fields between different tip speed ratios

Figure 12 conveys the fluctuations of wind velocity in upstream at longitudinal position x/R= -0.5 at two lateral positions (y/R= 0.2 and y/R= 1.0) in condition of different tip speed ratios. From the figure, fluctuation amplitudes inside rotor radius (y/R= 0.2) present the tendency of increase along with increasing tip speed ratio, at the same time azimuth angle corresponding to maximum amplitude also is ahead. Nevertheless, more complex fluctuations appear outside rotor radius (y/R= 1.0) than inside rotor radius (y/R= 0.2) during rotor rotation. Furthermore, fluctuations show the maximum value in the case of optimum tip speed ratio.

Figure 13 represents average velocity vector at different tip speed ratios in flow flied. The velocity distribution is substantially uniform at upstream side (x/R= -3.0) of wind turbines. Furthermore, approaching wind turbine in the upstream side of flow field at x/R= -1.5, the flow velocity decreases in the mainstream direction. The air flows outward to avoid the wind turbine as a result of the influence of the rotation of blades. Obviously, in mainstream direction, a



(a) $x/R<0$ (b) $x/R\geq 0$

Fig. 11 Lateral-wise Absolute Velocity Distribution (λ=1.03). Similar with Fig.10, velocity profile is also divided into two regions: upstream region ($x/R< 0$) and downstream region ($x/R\geq 0$). The vertical axe represents the non-dimensional wind velocity U_x/U_0 during the averaged flow field.

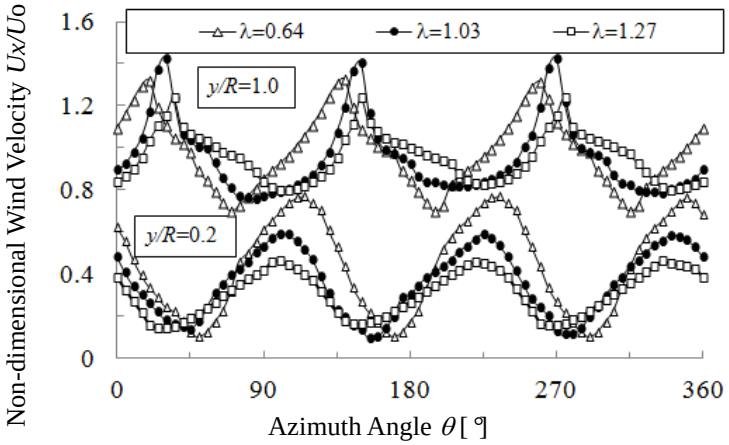
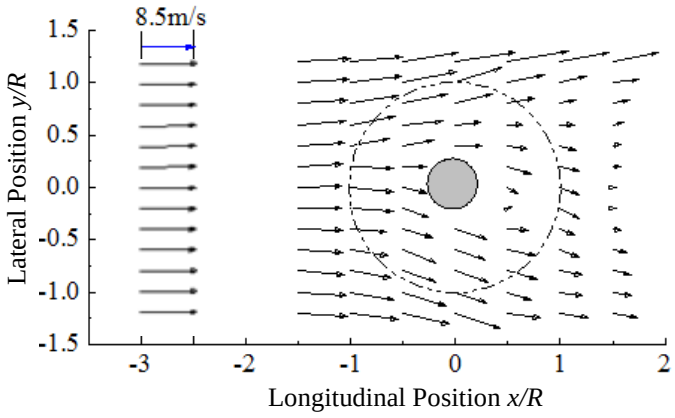


Fig. 12 Fluctuation of Wind Velocity for Different λ (x/R= -0.5). The three curves in the upside present fluctuation amplitudes at outer regions of the rotor (y/R=1.0) for different tip speed ratios. However, the three curves in the downside present fluctuation amplitudes at inner regions of the rotor (y/R=0.2) for different tip speed ratios.

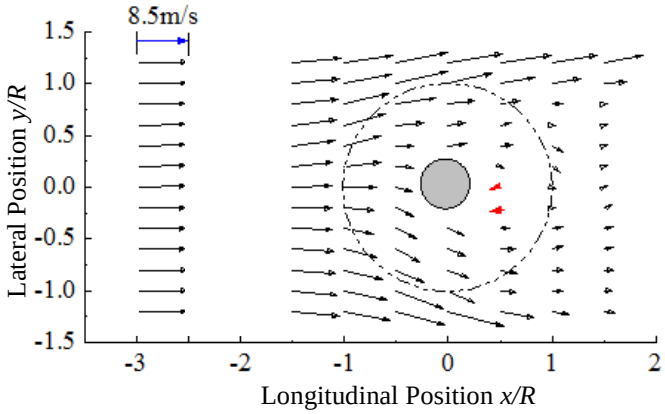
[DOI: 10.1299/jfst.2014jfst0051]
© 2014 The Japan Society of Mechanical Engineers

wide low wind velocity field appears from rotation region to downstream region of the wind turbine. Along with the increase of tip speed ratio, there is an expanding tendency of low wind velocity region. Meanwhile, it also must be noted that the reverse flow field which is indicated by red arrows only be generated in the back of the cover of the rotation axis (x/R = 0.5, y/R = 0 and -0.2) at the condition of optimum tip speed ratio. It seems that the main flow enables a quick recovery of the wake velocity which is mainly affected by the rotary axis at high tip speed ratio (λ=1.27).

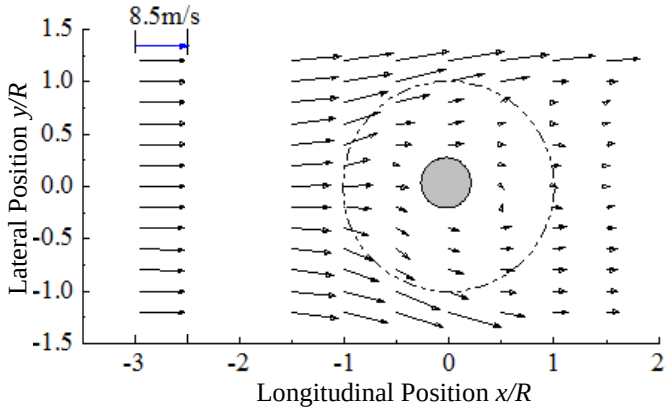
In the region of -1.2≤y/R≤1.2, the changes of stream-wise and lateral-wise averaged velocity are as shown in Fig. 14 and Fig. 15, respectively. However, in the section of x/R=0, the plotted velocities which are the averaged values do not include the measurement point of y/R=0 because the rotor shaft of the tested wind turbine is covered with a



(a) λ =0.64



(b) λ =1.03



(c) λ =1.27

Fig. 13 Average Velocity Distribution for Different λ. The length and direction of the arrows represent the value and direction of wind velocity, respectively. Small solid circle at x/R=0 and y/R=0, shows the cover portion of axis of rotation, and the red arrow represents the reverse flow.

[DOI: 10.1299/jfst.2014jfst0051]
© 2014 The Japan Society of Mechanical Engineers

cylindrical cover of 216 mm diameter. From Fig. 14, after entering rotor surface, stream-wise velocity is significantly reduced. As shown in Fig. 15, slight differences are found in the velocity change depending on tip speed ratio. Nonetheless, there is a large fluctuation inside rotor radius ($-1.0 \leq x/R \leq 1.0$). Lateral-wise wind velocity as well as stream-wise velocity show asymmetry caused by the rotor rotation. In addition, the lateral-wise wind velocity at upside regions of x-axis is larger than downside regions of x-axis. In this experiment, at the upstream position of x/R= -1.0 where the inflow just flows into the rotor area, the values of wind velocity deficit are 0.164, 0.242 and 0.274, for λ=0.64, 1.03 and 1.27, respectively; at the downstream position of x/R=1.0 where the inflow just flows out the surface of revolution, the values of wind velocity deficit are 0.566, 0.707 and 0.732, for λ=0.64, 1.03 and 1.27, respectively.

4.4 **Turbulence Intensity in Flow Field**

Figure 16 shows the change of turbulence intensities in the mainstream direction generated by optimum tip speed ratio (λ=1.03). The vertical axis represents the non-dimensional lateral coordinate, y/D. One division of scale in horizontal axis corresponds to the turbulence intensity of TI=0.5. Turbulence intensity, TI, which is defined as:

$$TI = \sigma / U_0 \tag{3}$$

where, U_0 and σ are the mainstream wind velocity and the standard deviation of local wind velocity, respectively.

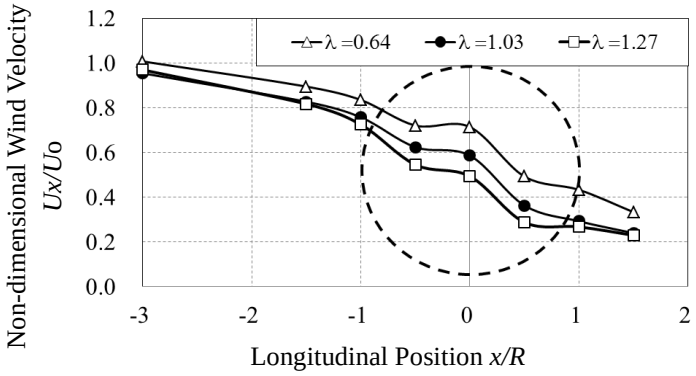


Fig. 14 Averaged Velocity along x-axis in Stream-wise Direction. The three curves represent average velocity vector at different tip speed ratios in every lateral position. The plotted velocities are the averaged values in the region of $-1.2 \leqslant y/R \leqslant 1.2$ (y/R= -1.2, -1.0, -0.8, -0.6, -0.4, -0.2, 0, 0.2, 0.4, 0.6, 0.8 1.0 and 1.2). However, in the section of x/R=0, the plotted velocities do not include the measurement point of y/R=0 because the rotor shaft of the tested wind turbine is covered with a cylindrical.

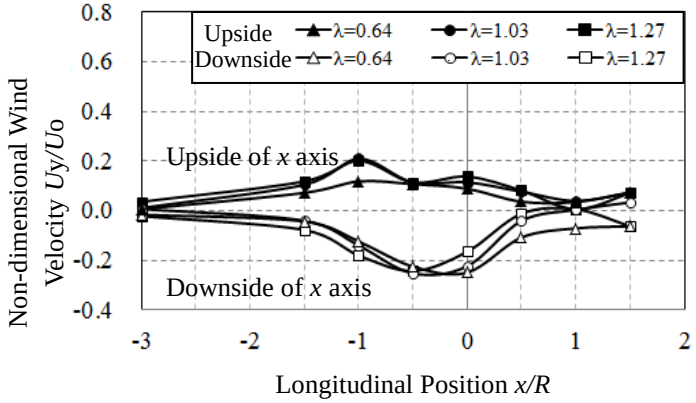


Fig. 15 Averaged Velocity along x-axis in Lateral-wise Direction. The change of velocity profile is divided into two regions: upside of x axis and downside of x axis. These curves represent average velocity vector at different tip speed ratios in every lateral position. The results for upside of x-axis and downside of x-axis are clearly distinguished by using different type of lines.

[DOI: 10.1299/jfst.2014jfst0051]
© 2014 The Japan Society of Mechanical Engineers

According to International Standard IEC 61400-12-1, standard deviation is the turbulent velocity fluctuations at every local measured point over a specified period of time (IEC 61400-12-1). In this research, the velocity fluctuations involve periodic and non-periodic components and the periodic fluctuation components should be excluded from evaluation of σ, so turbulent velocity fluctuations are described in terms of each azimuth angle of 5 ° BIN during one rotation. The standard deviation σ is defined as:

$$\sigma = \sqrt{\frac{1}{N}\sum_{i=1}^{N}(U_i - \overline{U})^2} \tag{4}$$

N is the number of data sample at each measurement point.

U_i is the local wind velocity at each azimuth angle of 5 °BIN during one rotation.

$\overline{U}$ is the averaged wind velocity at each measurement point during one rotation.

In general, the local mean wind velocity is used as the denominator in definition (3) for the wind assessment. However, here the mainstream wind velocity is used as the denominator in order to figure out not only the wind velocity deficit but also the wind velocity variance in flow field. It is clearly known that, in mainstream direction, large turbulence intensity appeared at the inside of wind turbine ($|x/R| \leq 1.0$).

Figure 17 shows the changes of stream-wise averaged turbulence intensity at different tip speed ratios, in the region of $-1.2 \leq y/R \leq 1.2$. As shown in Fig. 17, the turbulence decreases with the increase of tip speed ratio. For optimum tip speed ratio of λ=1.03, almost the same fluctuation can be seen as high tip speed ratio of λ=1.27. Furthermore, at the

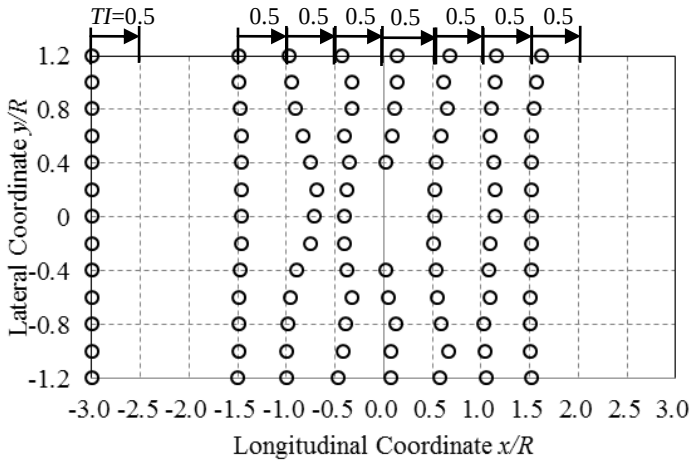


Fig. 16 Turbulence Intensity Distribution for λ=1.03. The change of turbulence intensities are shown in the mainstream direction at the optimum tip speed ratio. One division of scale in longitudinal coordination corresponds to the turbulence intensity of TI=0.5.

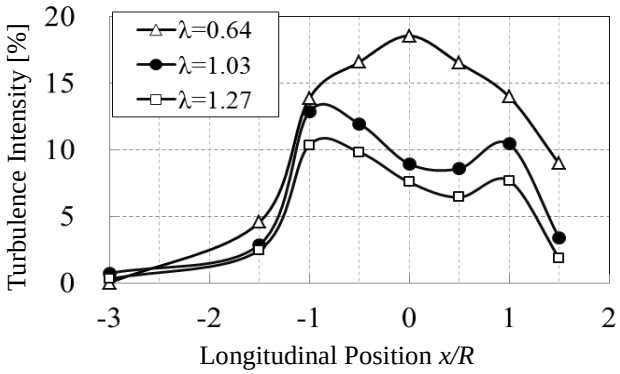


Fig. 17 Averaged Turbulence Intensity along x-axis Direction. The three curves represent average turbulence intensity at different tip speed ratios. Similar with Fig.10, the plotted turbulence intensity do not include the measurement point of y/R=0.

[DOI: 10.1299/jfst.2014jfst0051]
© 2014 The Japan Society of Mechanical Engineers

inside of wind turbine ($|x/R|\leq 1.0$), similar phenomenon does not appear in low tip speed ratio condition during rotor rotation. As for x/R= -1.0, the turbulence intensity reaches a maximum value, at λ=1.03 and 1.27. It seems that the result is due to large fluctuations of the tip speed velocity which exist there. However, the turbulence intensity reaches a maximum value, at x/R=0 when λ=0.64. Meanwhile, the turbulence enables a quicker recovery at high tip speed ratio of λ=1.27 than other tip speed ratios.

5. Conclusions

This paper is aimed at measuring velocity distribution in the whole flow field of small type straight-bladed VAWT, using LDV technologies. According to the wind tunnel experiments, flow field characteristics are obtained through measuring wind velocity at three different low speed ratios. And then, the following information is clarified by these measurements.

(1) Wind velocity in flow field indicates a periodic change depending on the rotation of the wind turbine. The fluctuations show opposite peaks at inner and outer regions of the rotor. Meanwhile, from upstream to downstream side, the velocity deficit has become greater in the mainstream direction.

(2) A wide low wind velocity field appears from rotation region to downstream region of the wind turbine. Along with the increase of tip speed ratio, the low wind velocity region is the trend of expansion.

(3) Velocity vector has an asymmetry with respect to the x-axis at the downstream side of the rotor the velocity. Variation is recovered in short distance in the wake (x/R=1.5) compared with stream-wise wind velocity. Lateral-wise absolute wind velocity is smaller than the stream-wise wind velocity. On the other hand, the reverse flow is only generated in the back of the cover of the rotation axis(x/R = 0.5, y/R = 0 and -0.2), at the condition of λ=1.03.

(4) In mainstream direction, large turbulence intensity appeared at the inside of wind turbine ($|x/R|\leq 1.0$). Meanwhile, the turbulence intensity decreases with increase of tip speed ratio.

6. Acknowledgments

First and foremost, this work is supported by New Energy and Industrial Technology Development Organization (NEDO) in Japan. Last but not least, my sincere appreciation also goes to my team members Kazuma Furukawa, Masayuki Yamamoto and Naohiro Maruyama, for their helpful assistance during the experiment.

References

Asress, M.B., Aleksandar, S., Dragan, K. and Slobodan, S., Numerical and analytical investigation of vertical axis wind turbine, Faculty of Mechanical Engineering Transactions, Vol.41 (2013), pp. 49-58.

Castelli, M.R., Fedrigo, A. and Benini, E., Effect of dynamic stall, finite aspect ratio and streamtube expansion on VAWT performance prediction using the BE-M model, World Academy of Science, Engineering and Technology, Vol.68 (2012), pp. 766-778.

Ferreira, C.S., van Kuik,G., van Bussel,G. and Scarano,F., Visualization by PIV of dynamic stall on a vertical axis wind turbine, Exp. Fluids (2009), pp.97–108.

Fujisawa, N. and Shibuya, S., Observations of dynamic stall on darrieus wind turbine blades, Journal of Wind Engineering and Industrial Aerodynamics, Vol.89 (2001), pp. 201-214.

IEC61400-12-1, Wind turbine part 1: design requirements, IEC TC88-MT1 ed (2005), p.92.

Maeda,T., Kamada,Y., Murata, J., Li, Q., Kawabata, T. and Kogaki, T., Measurements of flow field and pressure distribution of straight-bladed vertical axis wind turbine, Proc. European Wind Energy Association Conference and Exhibition (2013), p.8.

Mazharul, I., David, S.K. and Amir, F., Aerodynamic models for darrieus-type straight-bladed vertical axis wind turbines, Renewable and Sustainable Energy Reviews, (World Academy of Science, Engineering and Technology), Vol. 12 (2008), pp. 1087-1109.

Rajat, G., Sukanta, R. and Agnimitra, B., Computational fluid dynamics analysis of a twisted airfoil shaped two-bladed

[DOI: 10.1299/jfst.2014jfst0051]
© 2014 The Japan Society of Mechanical Engineers

H-Darrieus rotor made from fibreglass reinforced plastic (FRP), International Journal of Energy and Environment, Vol. 1, Issue 6 (2010), pp.953-968.

Sato, Y., Okazaki, H., Shoda, T., Nishio, Y., Shigeta, M. and Izawa, S., Hotwire measurement and numerical analysis of flows around a straight wing vertical axis wind turbine, Transactions of the Japan Society of Mechanical Engineers, Series B, Vol.77, No.775 (2011), pp.637-646 (in Japanese).

[DOI: 10.1299/jfst.2014jfst0051]
© 2014 The Japan Society of Mechanical Engineers